Aerodynamic Challenges of Major Chinese Bridges

Yao Jun GE
Professor
State Key Lab for Disaster Reduction in Civil Eng.
Tongji University
Shanghai, 200092, China
yaojunge@mail.tongji.edu.cn

Yao Jun Ge, born 1958, received his PhD degree in bridge engineering from Tongji University. He is currently Chairman of the Department of Bridge Engineering.

Hai Fan XIANG
Emeritus Professor
College of Civil Engineering
Tongji University
Shanghai, 200092, China
hfxiang@mail.tongji.edu.cn

Hai Fan Xiang, born 1935, received his MSc degree in bridge engineering from Tongji University. He is currently the Consulting Dean of the College of Civil Engineering.

Summary

This paper presents recent advances in aerodynamic studies of flutter instability, vortex induced vibration, and stay cable vibration, undertaken to address the most formidable challenges of long-span bridge design. Aerodynamic stabilization for long-span suspension bridges is introduced, followed by an aerodynamic feasibility study of a 5 000 m-span suspension bridge. It seems that the intrinsic limit of span length due to aerodynamic stability is about 1 500 m for a traditional suspension bridge, but either a widely slotted deck or a narrowly slotted deck with vertical and horizontal stabilizers could provide a 5 000 m suspension bridge with high enough critical flutter speed. Since cable-stayed bridges have good intrinsic aerodynamic stability, rain-wind induced vibration and mitigation are discussed as the primary concern encountered in the design of most long-span cable-stayed bridges. It is possible to increase the span length of cable-stayed bridges in the near future while ensuring aerodynamic stability. Compared to suspension bridges and cable-stayed bridges, arch bridges have relatively shorter span and higher stiffness. Consequently, only one of the ten longest-span arch bridges, namely Shanghai's Lupu Bridge, suffers vortex-induced vibration as described in the paper. An increase in span length of arch bridges should not be influenced by aerodynamic requirements.

Keywords: Suspension bridge, cable-stayed bridge, arch bridge, flutter stability, vortex-shedding vibration, rain-wind induced vibration

1. Introduction

Since the implementation of China's reform and open-door policy in 1978, the country's economy has soared for the past three decades with 9% average annual growth rate of Gross Domestic Product. This has created a great demand for development of transportation infrastructure, in particular the country's highway system. During the golden period of highway construction that began in 1988, unprecedented development of highway bridge construction has been experienced in the country. By the end of 2008, the total number of highway bridges will increase to 550 000, for a total length of 21 000 km. Both figures represent an almost fourfold increase since 1988. Among these highway bridges are numerous long-span bridges, whose construction began with the great success of Shanghai's Nanpu Bridge (Fig. 1a) completed in 1991, whose cable-stayed span of 423 m was then the third longest in the world. By the end of 2008, there were 51 long-span bridges with a main span over 400 m in China, including 16 suspension bridges, 28 cable-stayed bridges, and 7 arch bridges. These are listed in Table 1 (Xiang, Chen & Ge, 2003). Shanghai's Lupu Bridge (Fig. 1b) with a 550 m main span holds the world record span length for arch bridges. The main span lengths of cable-supported bridges include the 1088 m span of the Jiangsu Sutong Bridge (Fig. 1c), the longest cable-stayed bridge span in the world, and the 1650 m span of the Zhejiang Xihoumen Bridge (Fig. 1d), the longest box-girder suspension bridge span in the world (Ge & Xiang, 2006a).

TABLE 1

CHINESE LONG-SPAN BRIDGES WITH MAIN SPAN OVER 400 m

Type	No	Bridge Name	Main Span	Year Built	No	Bridge Name	Main Span	Year Built
Suspension	1	Tibet Dazi	500 m	1984	9	Sichuan Egongyan	600 m	2000
	2	Shantou Bay	452 m	1995	10	Sichuan Zhongxian	560 m	2001
	3	Hubei Xiling	900 m	1996	11	Hubei Yicang	960 m	2001
	4	Sichuan Fengdu	450 m	1997	12	2nd Sichuan Wanxian	580 m	2004
	5	Guangdong Humen	888 m	1997	13	Jiangsu Runyang S.	1490 m	2005
	6	Hong Kong Tsing Ma	1377 m	1997	14	Hubei Yangluo	1280 m	2007
	7	Xiamen Haicang	648 m	1999	15	Guangdong Huangpu	1108 m	2008
	8	Jiangsu Jiangyin	1385 m	1999	16	Zhejiang Xihoumen	1650 m	2008
Cable-Stayed	1	Shanghai Nanpu	423 m	1991	15	Hubei Jingzhou	500 m	2002
	2	Hubei Yunyan	414 m	1993	16	Hubei Ehuang	480 m	2002
	3	Shanghai Yangpu	602 m	1993	17	Zhejiang Taoyaomen	580 m	2003
	4	Anhui Tongling	432 m	1995	18	Fujian Qingzhou	605 m	2003
	5	2nd Hubei Wuhan	400 m	1995	19	Anhui Anqing	510 m	2004
	6	Chongqing Lijiatuo	444 m	1996	20	East Sea Main Bridge	420 m	2005
	7	Shanghai Xupu	590 m	1997	21	3rd Jiangsu Nanjing	648 m	2005
	8	H.K. Kap Shui Mun	430 m	1997	22	Jiangsu Runyang N.	406 m	2005
	9	Hong Kong Ting Kau	475 m	1998	23	Zhanjiang Bay	480 m	2007
	10	Hubei Queshi	518 m	1999	24	Hangzhou Bay	448 m	2008
	11	Hubei Baishazhou	618 m	2000	25	Sichuan Fuling	450 m	2008
	12	Chongqing Dafosi	450 m	2001	26	Hubei Tianxinzhou	504 m	2008
	13	2nd Jiangsu Nanjing	628 m	2001	27	Zhejiang Jintang	620 m	2008
	14	Hubei Junshan	460 m	2002	28	Jiangsu Sutong	1088 m	2008
Arch	1	Sichuan Wanxian	420 m	2001	5	Chongqing Caiyuanba	420 m	2008
	2	Shanghai Lupu	550 m	2003	6	Guangdong Xinguang	428 m	2008
	3	Sichuan Wushan	460 m	2005	7	Chongqing Caotianmen	552 m	2008
	4	4th Hunan Xiantan	400 m	2007				

With this rapid increase of bridge span length, bridge structural systems are becoming more flexible. This requires aerodynamic studies related to flutter instability, vortex induced vibration, stay cable vibration, and other aspects of dynamic behaviour. This paper discusses the aerodynamic stabilization of several suspension bridges recently built in China and presents an aerodynamic feasibility study of a 5000 m span suspension bridge. Since cable-stayed bridges intrinsically have good aerodynamic stability against flutter oscillation, rain-wind induced vibration and mitigation are discussed as a main concern in the design of most long-span cable-stayed bridges. Compared to suspension bridges and cable-stayed bridges, arch bridges have relatively shorter spans and higher stiffness. Long-span arch bridges will generally not have wind-induced problems except for Shanghai’s Lupu Bridge that experienced vortex-induced vibration.

(a) Shanghai Nanpu Bridge

(b) Shanghai Lupu Bridge

(c) Jiangsu Sutong Bridge

(d) Zhejiang Xihoumen Bridge

Figure 1: The first and longest span bridges in China

2. Aerodynamic Stabilization of Suspension Bridges

The construction of long-span suspension bridges around the world has experienced considerable development over the past century. Beginning with the 483 m span of the Brooklyn Bridge, built in 1883, the main span length of suspension bridges increased to 1280 m with the construction of the Golden Gate Bridge in 1937, i.e., by a factor 2.7 over 54 years. For the next 44 years, the incrase slowed to a factor of 1.1, following completion of the Humber Bridge's main span of 1 410 m in 1981. Completion in 1998 of the Akashi Kaikyo Bridge, with a main span of 1 991 m, represents an increase by a factor of 1.4 over 17 years.

TABLE 2

TEN LONGEST-SPAN SUSPENSION BRIDGES IN THE WORLD

Span Order	Bridge Name	Main Span	Girder Type	Wind-Induced Problem	Control Measure	Country	Year Built
1	Akashi Kaikyo	1991 m	Truss	Flutter	Slot/Stabilizer	Japan	1998
2	Zhejiang Xihoumen	1650 m	Box	Flutter	Slot	China	2008
3	Great Belt	1624 m	Box	Vortex	Guide vane	Denmark	1998
4	Jiangsu Runyang S.	1490 m	Box	Flutter	Stabilizer	China	2005
5	Humber	1410 m	Box	None	None	U.K.	1981
6	Jiangsu Jiangyin	1385 m	Box	None	None	China	1999
7	Hong Kong Tsing Ma	1377 m	Box	Flutter	Slot	H.K. China	1997
8	Verrazano	1298 m	Truss	None	None	U.S.A.	1964
9	Golden Gate	1280 m	Truss	None	None	U.S.A.	1937
10	Hubei Yangluo	1280 m	Box	None	None	China	2007

The ten longest span suspension bridges in the world are listed in Table 2, including five in China, two in the USA, and one each in Japan, Denmark, and the UK (Internet address A, 2007). Table 2 provides not only general figures about span, year of completion and location, but also specific information related to wind resistance performance, including girder type, wind-induced problem, and control measure adopted. The top four suspension bridges in Table 2 were all susceptible to wind-induced problems in flutter or vortex shedding, and control measures were adopted to improve aerodynamic performance. These measures included a central stabilizer for the Jiangsu Runyang South Bridge, a twin-box deck for the Zhejiang Xihoumen Bridge, both a slot and a stabilizer for the Akashi Kaikyo Bridge, and a guide vane for the Great Belt Bridge.

2.1 Single Box Girder with Central Stabilizer

The Jiangsu Runyang South Bridge, completed in 2005, is the second longest suspension bridge in China and the fourth longest in the world. The bridge connects Zhenjiang City and Yangzhou City over the Yangtze River in the eastern Chinese province of Jiangsu. The main section of the bridge was designed as a typical three-span suspension bridge with a span arrangement of 510 m + 1490 m + 510 m as shown in Fig. 2. The deck cross section is a traditional closed steel box, 36.3 m wide and 3 m deep, and carries three 3.75 m wide traffic lanes in each direction with 3.5 m wide shoulders on both sides for emergencies (Fig. 3). The box girder is equipped with classical barriers and sharp fairings intended to improve aerodynamic streamlining as well as aesthetic quality (Chen et al., 2002).

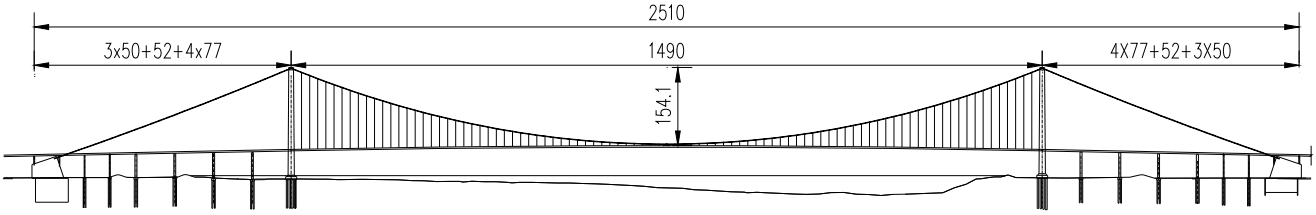

Figure 2: Elevation of the Jiangsu Runyang South Bridge (Dimensions in m)

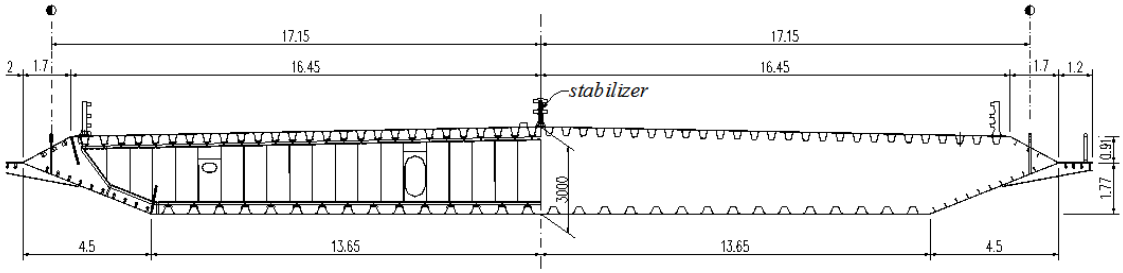

Figure 3: Deck cross-section of the Jiangsu Runyang South Bridge (Dimensions in m)

TABLE 3

FUNDAMENTAL NATURAL FREQUENCIES OF BOX GIRDER SUSPENSION BRIDGES

Bridge Name	Span (m)	Lateral Frequency (Hz)		Vertical Frequency (Hz)		Torsional Frequency (Hz)	
		Symmetric	Antisymm.	Symmetric	Antisymm.	Symmetric	Antisymm.
Runyang	1490	0.0489	0.1229	0.1241	0.0884	0.2308	0.2698
Great Belt	1624	0.0521	0.1180	0.0839	0.0998	0.2780	0.3830
Xihoumen	1650	0.0484	0.1086	0.1000	0.0791	0.2323	0.2380

With the structural properties provided in the reference (Chen et al., 2002), finite element analysis of the dynamic characteristics of the prototype bridge was performed, and the symmetrical and antisymmetrical fundamental natural frequencies of lateral, vertical, and torsional vibration modes were calculated and compared with those of other box-girder suspension bridges, including the Great Belt Bridge and the Zhejiang Xihoumen Bridge in Table 3. The fundamental vertical and lateral vibration frequencies of the Jiangsu Runyang South Bridge are reasonable, but the torsional vibration frequencies are relatively lower than those of the other two bridges mainly because of the small depth of the box section.

To study the aerodynamic stability, a wind tunnel experiment with a 1:70 sectional model was carried out in the TJ (Tongji University) -1 Boundary Layer Wind Tunnel with a working section 1.8 m wide, 1.8 m high, and 15 m long. It was found in the first phase of testing that the original structure could not meet the requirement of flutter speed of 54 m/s. Some preventive means thus had to be considered to stabilize the original structure. Further sectional model testing was conducted with a stabilizer arranged along the centreline of the deck as shown in Fig. 3. Confirmation wind tunnel tests with a full aeroelastic model were also performed in the TJ-3 Wind Tunnel with a working section 15 m wide, 2 m high, and 14 m long. The critical flutter speeds obtained from the sectional model (SM) and full model (FM) wind tunnel tests are collected and compared in Table 4. Both experimental results show good agreement with each other, and validate that the central stabilizer of 0.88 m height as shown in Fig. 4 can raise the critical flutter speed over the required value (Chen et al., 2002).

TABLE 4
CRITICAL FLUTTER SPEEDS OF THE JIANGSU RUNYANG SOUTH BRIDGE

Box Girder Configuration	Critical flutter speed (m/s)				Required (m/s)
	SM at 0°	FM at 0°	SM at +3°	FM at +3°	
Original box girder	64.4	64.3	50.8	52.5	54
Box girder with a 0.65m stabilizer		69.5	58.1	53.8	54
Box girder with a 0.88m stabilizer		72.1	64.9	55.1	54
Box girder with a 1.1m stabilizer		>75	67.4	56.4	54

Figure 4: Central stabilizer mounted on the Jiangsu Runyang South Bridge

2.2 Twin Box Girder with Central Slot

The Zhejiang Xihoumen Bridge will become the longest suspension bridge in China and the second longest in the world behind the Akashi Kaikyo Bridge. This bridge is part of the Zhoushan Island-Mainland Connection Project linking the two islands of Jintang and Cezi in Zhejiang Province. It crosses the Xihoumen Strait, one of the most important national deep waterways. The bridge route was selected at the narrowest point of the Xihoumen Strait, where the distance between Jintang and Cezi is about 2200 m and where a small island near Cezi, Tiger Island, can be used to support a pylon for a cable-supported bridge. The other pylon is located on the slope forming the shore of Jintang Island. The precise location of the pylon foundation on Jintang was the subject of a detailed study, with consideration of its effect on main span length. A foundation above the water level with main span of 1650 m, a foundation 20 m under water with a main span of 1520 m, and a foundation 35 m under water with a main span of 1310 m were among the combinations studied. To avoid constructing deep-water foundations, the Xihoumen Bridge was finally designed as a suspension bridge two suspended spans and a main span of 1650 m, as shown in Fig. 5 (China Highway Planning and Design Institute, 2003).

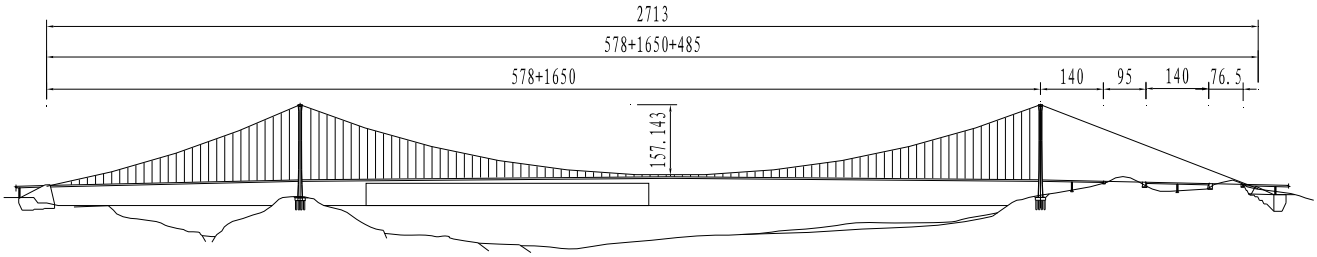

Figure 5: Elevation of the Zhejiang Xihoumen Bridge (Dimensions in m)

Based on the experience gained from the 1490 m Runyang Bridge with flutter speed of 51 m/s and the 1624 m Great Belt Bridge with flutter speed of 65 m/s, problems with aerodynamic instability were anticipated for the span length of 1650, even with the stricter stability requirement of 78.4 m/s for the Xihoumen Bridge. Four alternative configurations of box girders were proposed and were investigated through sectional model wind tunnel tests. Apart from the traditional single box, the other three deck sections, including a single box with a central stabilizer of 2.2 m (Fig. 6a) and twin box decks with a central slot of 6 m (Fig. 6b) or 10.6 m (Fig. 6c), satisfied the flutter stability requirement shown in Table 5. The 6 m slotted twin-box girder was adopted, which was further modified to the final configuration as shown in Fig. 6d (Ge et al., 2003).

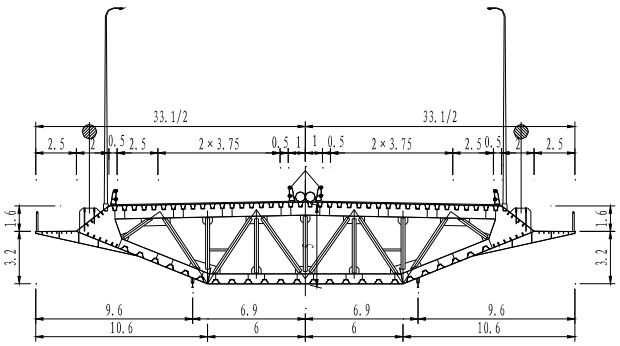

(a) Single box

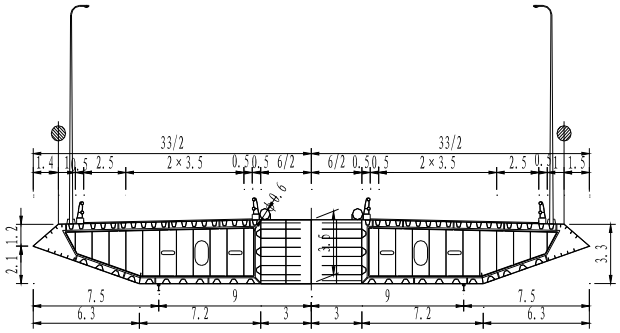

(b) Twin box with a 6 m slot

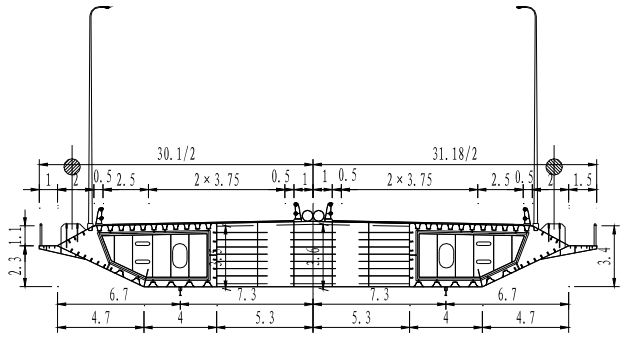

(c) Twin box with a 10.6 m slot

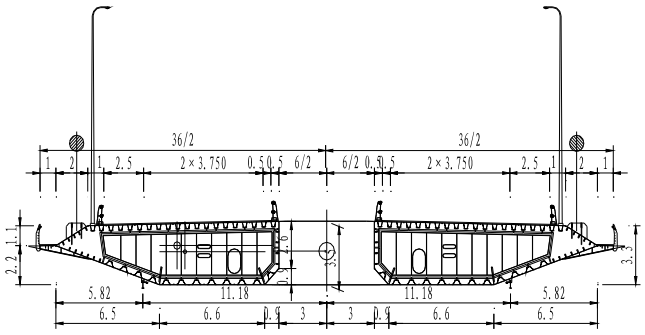

(d) Final scheme

Figure 6: Proposed box girder sections for the Zhejiang Xihoumen Bridge (Dimensions m)

TABLE 5

CRITICAL FLUTTER SPEEDS OF THE ZHEJIANG XIHOUMEN BRIDGE

Deck Box Girder Configuration	Critical flutter speed (m/s)				Required (m/s)
	–3°	0°	+3°	Minimum	
Single box girder	50.7	46.2	48.7	46.2	78.4
Single box with a 1.2m stabilizer	>89.3	>89.3	37.7	37.7	78.4
Single box with a 1.7m stabilizer	88.0	>89.3	43.4	43.4	78.4
Single box with a 2.2m stabilizer	>89.3	>89.3	88.0	88.0	78.4
Twin box with a slot of 6m	88.4	>89.3	>89.3	88.4	78.4
Twin boxes with a slot of 10.6m	>89.3	>89.3	>89.3	>89.3	78.4

2.3 Stabilization for Super Long Spans

As a long-time dream and an engineering challenge, the technology of bridging larger obstacles has entered into a new era of crossing wider sea straits. Examples of these bridge sites include, for example, the Messina Strait in Italy, the Qiongzhou Strait in China, the Tsugaru Strait in Japan, and the Gibraltar Strait linking the European and African Continents. One of the most interesting challenges in this regard has been to determine the limit of suspension bridge span length. The dominant concerns in the design of super long span bridges are technological feasibility and aerodynamic considerations. From the perspective of aerodynamic stabilization for longer span lengths, a typical three-span suspension bridge with a 5 000 m central span and two 1 600 m side spans is considered to be the effective limit of span length (Fig. 7).

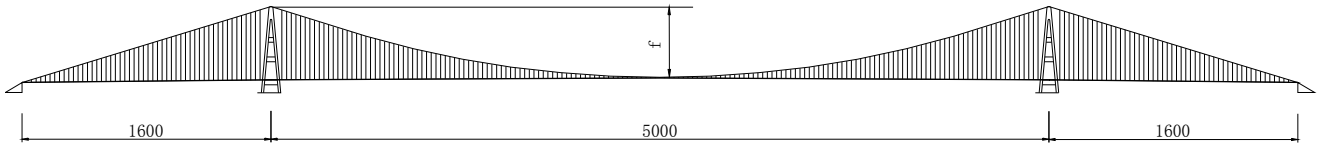

Figure 7: Elevation of the 5 000 m long suspension bridge (Dimensions in m)

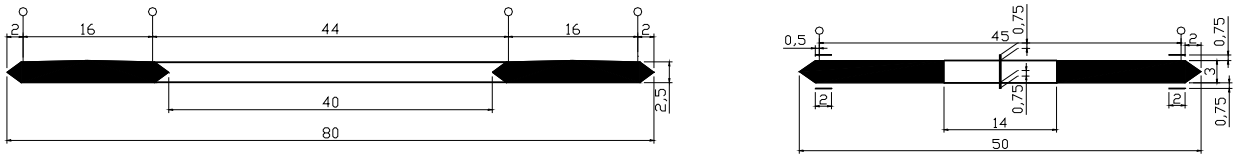

(a) WS Cross section (b) NS Cross section

Figure 8: Geometry of deck sections of WS and NS (Dimensions in m)

In order to increase the limit of aerodynamic stability, two kinds of generic deck sections, namely a wide slotted deck (WS) without stabilizers (Fig. 8a) and a narrow slotted deck with vertical and horizontal stabilizers (NS) (Fig. 8b), were investigated. The WS cross section has a total deck width of 80 m and four main cables for a 5 000 m span; the NS provides a deck width of 50 m and two main cables (Xiang & Ge, 2003; Ge & Xiang, 2006b).

Having performed a dynamic finite-element analysis based on the structural parameters listed in Table 6, the fundamental natural frequencies of the structures have been calculated for four ratios n of cable sag to span and the two deck configurations shown in Table 7. The fundamental lateral bending frequencies vary by about 16% for the WS section and 17% for the NS section from n =1/8 to n =1/11, but remain practically identical for both the WS and the NS deck configurations. The fundamental vertical bending frequencies are not influenced significantly by either deck configuration or sag-span ratio. The fundamental torsional frequencies vary differently with ratio n in the two deck configurations. This frequency increases in the WS section and decreases in the NS section with decreasing n. For both deck configurations, the ratio of torsional frequency to bending frequency decreases with decreasing n.

TABLE 6

PARAMETERS OF STIFFNESS AND MASS OF THE 5 000 m SUSPENSION BRIDGE

Section	Main Cables			Stiffening Girder			
	EA (Nm^2)	m (kg/m)	I_m (kgm^2/m)	EI_y (Nm^2)	GI_d (Nm^2)	m (kg/m)	I_m(kgm^2/m)
WS	$0.61\sim1.12\times10^6$	$2.62\sim4.82\times10^4$	$2.36\sim4.33\times10^7$	4.7×10^{11}	2.8×10^{11}	24000	2.16×10^7
NS	$0.61\sim1.12\times10^6$	$2.62\sim4.82\times10^4$	$1.27\sim2.33\times10^7$	8.1×10^{11}	4.1×10^{11}	24000	5.40×10^6

TABLE 7

FUNDAMENTAL NATURAL FREQUENCIES OF THE 5 000 m SUSPENSION BRIDGE

Ratio	Lateral (Hz)		Vertical (Hz)		Torsional (Hz)		Frequency Ratio	
	WS	NS	WS	NS	WS	NS	WS	NS
n = 1/8	0.02199	0.02156	0.05955	0.05936	0.07090	0.09073	1.191	1.528
n = 1/9	0.02322	0.02285	0.06126	0.06115	0.07207	0.08928	1.176	1.460
n = 1/10	0.02438	0.02406	0.06219	0.06204	0.07268	0.08653	1.168	1.395
n = 1/11	0.02548	0.02520	0.06237	0.06219	0.07269	0.08403	1.165	1.351

TABLE 8

CRITICAL FLUTTER WIND SPEEDS OF THE 5 000 m SUSPENSION BRIDGE

Ratio	m ($\times 10^4$kg/m)		I_m ($\times 10^7$kgm^2/m)		f_h (Hz)		f_α (Hz)		U_{cr} (m/s)	
	WS	NS	WS	NS	WS	NS	WS	NS	WS	NS
n = 1/8	6.01	6.79	5.28	2.37	0.05955	0.05936	0.07090	0.09073	82.9	74.7
n = 1/9	6.27	7.43	5.36	3.22	0.06126	0.06115	0.07207	0.08928	88.8	77.4
n = 1/10	6.73	8.33	5.92	3.29	0.06219	0.06204	0.07268	0.08653	90.9	78.9
n = 1/11	7.66	9.52	6.77	3.62	0.06237	0.06219	0.07269	0.08403	98.9	82.7

With the dynamic characteristics given above and the numerically identified flutter derivatives, the critical wind speeds of the suspension bridges were calculated by multi-mode flutter analysis assuming a structural damping ratio of 0.5%. The results of critical wind speeds together with the generalized mass and mass moment of inertia are summarized in Table 8. For both deck sections the critical wind speed increases with decreasing values of n, although the ratio of torsional frequency to vertical bending frequency decreases slightly. The most important reason for this behaviour is the considerable increase of the generalized properties in the aerodynamic stability analysis. The minimum critical wind speeds for the WS and NS sections are 82.9 m/s and 74.7 m/s, respectively (Ge & Xiang, 2006a; Ge & Xiang, 2007).

3. Aerodynamic Concerns of Cable-Stayed Bridges

Cable-stayed bridges can be traced back to the 18th century. Many early suspension bridges were of hybrid suspension and cable-stayed construction, such as the Brooklyn Bridge. One of the first modern cable-stayed bridges was a concrete-decked structure built in 1952 over the Donzere-Mondragon Canal in France, but it had little influence on later development. The steel-decked Stromsund Bridge, designed by Franz Dischinger and built in Sweden in 1955 with a main span of 183 m, is therefore more often cited as the first modern cable-stayed bridge. It took 31 years for the span length of cable-stayed bridges to increase to 465 m with the construction of the Annacis Bridge in Canada in 1986. In the last decade of the twentieth century, record span length increased rapidly. Notable examples of record spans are the 1991 Skarnsund Bridge (520 m), the 1993 Yangpu Bridge (602 m), the 1995 Normandy Bridge (856 m) and the 1999 Tatara Bridge (890 m). With the completion of the 1088 m main span of the Jiangsu Sutong Bridge in 2008, the record increased again by almost 200 m.

Table 9 lists the ten longest-span cable-stayed bridges in the world, to which China has contributed eight, and Japan and France have made one contribution each (Internet address B, 2007). Except for the Fujian Qingzhou Bridge which were susceptible to aerodynamic instability because of its bluff composite deck, almost all other cable-stayed bridges listed in Table 9 were susceptible to stay cable vibration induced by wind and rain condition, and adopted one or two vibration control measures, including dimples or spiral wires on cable surface, and mechanical dampers at the low ends of cables.

TABLE 9

TEN LONGEST-SPAN CABLE-STAYED BRIDGES IN THE WORLD

Span Order	Bridge Name	Main Span	Girder Type	Wind-Induced Problem	Control Measure	Country	Year Built
1	Jiangsu Sutong	1088 m	Steel box	Stay cables	Dimples/Damper	China	2008
2	Tatara	890 m	Steel box	Stay cables	Dimples/Damper	Japan	1999
3	Normandy	856 m	Steel box	Stay cables	Spiral-wires/Damper	France	1995
4	3rd Jiangsu Nanjing	648 m	Steel box	Stay cables	Dimples/Damper	China	2005
5	2nd Jiangsu Nanjing	628 m	Steel box	Stay cables	Spiral-wires/Damper	China	2001
6	Zhejiang Jintang	620 m	Steel box	Stay cables	Spiral-wires/Damper	China	2008
7	Hubei Baishazhou	618 m	Steel box	Stay cables	Dimples/Damper	China	2000
8	Fujian Qingzhou	605 m	Π girder	Flutter	Guide vane	China	2003
9	Shanghai Yangpu	602 m	Π girder	Stay cables	Damper	China	1993
10	Shanghai Xupu	590 m	Steel box	None	Damper	China	1997

3.1 Record-Breaking Cable-Stayed Bridges

The cable-stayed bridge has become the most popular type of long-span bridge in China for the past two decades. In 1993, Shanghai's Yangpu Bridge with a main span of 602 m became the longest span cable-stayed bridge in the world for a brief time. Although this record was quickly surpassed by the Normandy Bridge in 1995 and the Tatara Bridge in 1999, China already has about 30 cable-stayed bridges with main span longer than 400 m, and is currently constructing three record-breaking span length cable-stayed bridges, including the recently completed 1088 m Jiangsu Sutong Bridge as well as the 1018 m Stonecutters Bridge in Hong Kong and the 926 m Hubei Edong Bridge to be completed respectively in 2009 and 2010 (Ge & Xiang, 2007).

The Jiangsu Sutong Bridge, connecting the cities of Suzhou and Nantong over the Yangtze River in eastern China, consists of seven steel deck spans including a 1088 m long central span and three spans of 300 m + 100 m + 100 m on both sides as shown in Fig. 9. The cross-section of the deck is a streamlined orthotropic steel box, 35.4 m wide and 4 m deep, with two vertical webs required by the longitudinal load distribution. This box-girder carries three 3.75 m wide lanes of traffic in each direction with 3.5 m wide hard shoulders for emergency as shown in Fig. 10. The erection of the steel deck was completed in June 2007, and the bridge was opened to traffic in May 2008 (Pei et al., 2004).

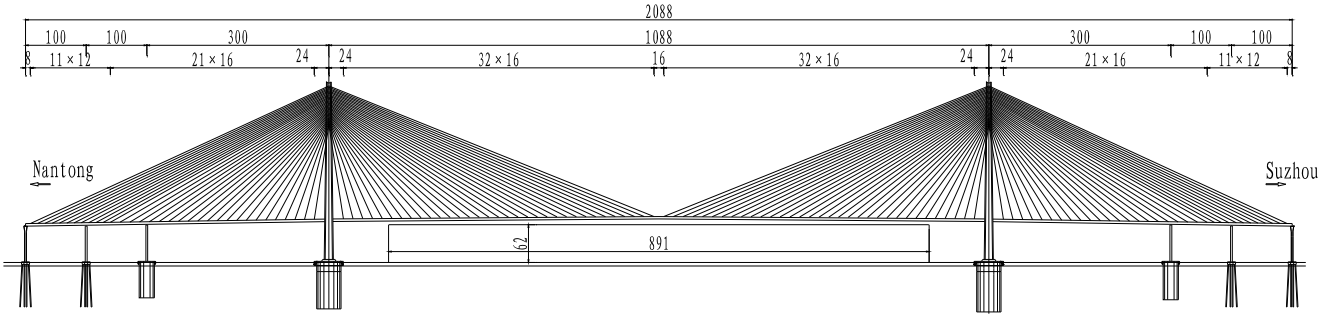

Figure 9: Elevation of the Jiangsu Sutong Bridge (Dimensions in m)

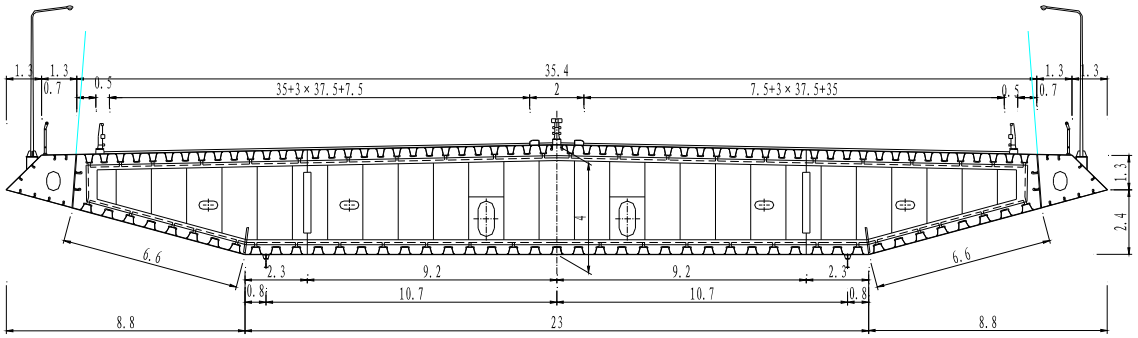

Figure 10: Deck cross-section of the Jiangsu Sutong Bridge (Dimensions in m)

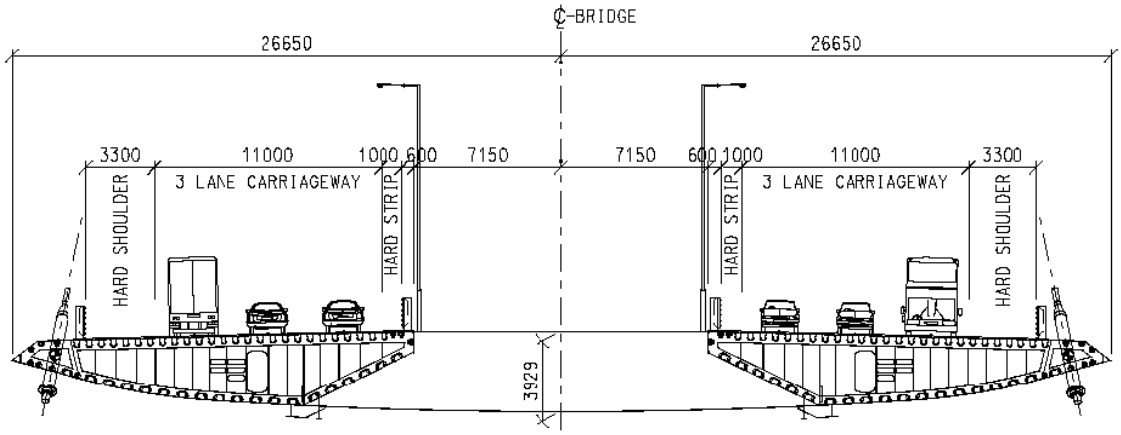

Figure 11: Deck cross-section of the Stonecutters Bridge in Hong Kong (Dimensions in mm)

The Stonecutters Bridge in Hong Kong is composed of nine spans including a 1018 m long central span with steel deck and four spans of 79.75 m + 70 m + 70 m + 69.25 m on both sides with concrete deck. The cross-section of the steel deck is made up of twin streamlined orthotropic steel boxes, 2×15.9 m wide and 3.9 m deep. This twin box girder carries three traffic lanes of 11 m width in each direction with 3.3 m wide hard shoulders for emergency parking as shown in Fig. 11. The bridge is scheduled to be completed by mid-2009 (Falbe-Hansen et al., 2004).

The Hubei Edong Bridge over the Yangtze River is a nine span hybrid cable-stayed bridge with a 926 m long central span with steel deck and four spans of 85 m + 65 m + 65 m + 65 m on both sides with concrete deck. Following a comparison of dynamic and aerodynamic characteristics with a traditional closed box, the cross-section of the steel deck was designed as two separate box girders with total deck width of 34.4 m and depth of 3.8 m, without the bottom plate in the central part to save material, as shown in Fig. 12. The two pylons of this bridge are currently under construction, and the bridge will be finished by early 2010 (Song et al., 2005).

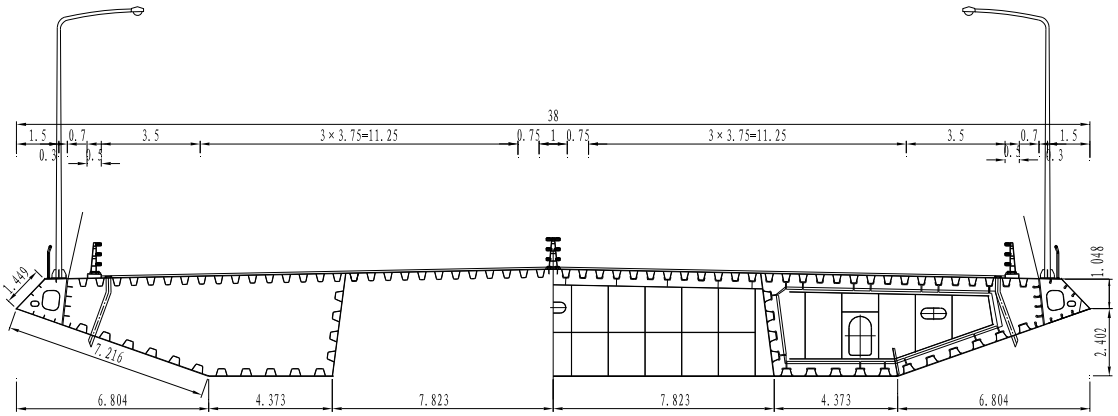

Figure 12: Deck cross-section of the Hubei Edong Bridge (Dimensions in m)

3.2 Critical Flutter Speed

There were two great moments in the history of cable-stayed bridges when the record span increased dramatically. The first was in 1995, with the 254 m leap from the 602 m span of the Yangpu Bridge to the 856 m span of the Normandy Bridge. The second was in 2008 with the 198 m increase of the record from the 890 m span of the Tatara Bridge to the 1088 m span of the Sutong Bridge. Is it possible to make further significant increases of the span length of cable-stayed bridges? Apart from structural materials and construction technology, among the most important concerns related to this question are dynamic and aerodynamic characteristics.

In order to study the dynamic characteristics of a cable-stayed bridge, the finite-element method is generally used to calculate the natural frequencies of an idealized structure. The finite-element idealization of a cable-stayed bridge is basically created with beam elements for longitudinal girders, transverse beams and pylon elements, and cable elements that account for the geometric stiffness of stay cables. Dimensions and material properties should be correctly provided for all structural components. Having performed a dynamic finite-element analysis, the first several natural frequencies of the cable-stayed bridge can be found, including those related to the lateral bending, vertical bending,

and torsional modes. The fundamental frequencies of the lateral bending, vertical bending, and torsional modes of five cable-stayed bridges with a main span over 800 m are collected and compared in Table 10 (Ge & Xiang, 2007). Among these five bridges, the Tatara Bridge is an exceptional case with the smallest values of the fundamental frequencies. This is due to the relatively small depth and width of the box girder. This bridge also has the largest ratio of torsional frequency to vertical frequency. With its unique twin box girder, the Stonecutters Bridge has the next smallest fundamental frequencies of lateral and vertical bending modes. Its torsional frequency is almost the same as those of the Tatara Bridge and the Normandy Bridge. As the longest cable-stayed bridge, the Sutong Bridge even has the highest torsional frequency all five bridges. It should be concluded that there is no clear tendency with regard to fundamental frequencies of cable-stayed bridges as a function of span length.

The most important aerodynamic characteristic is flutter instability, which can be evaluated by simply comparing critical flutter speed with required wind speed. Critical flutter speed of a bridge can be determined through a direct experimental method, using a sectional model or a full aeroelastic model, as well as computationally using experimentally identified flutter derivatives. Required wind speed is based on basic design wind speed multiplied by modification factors to account for deck height, gust speed, longitudinal correlation of wind speed, safety factor of flutter, and so on. Both the critical flutter speeds and the required wind speeds of these five bridges are shown in Table 10. It is surprising to see that both critical flutter speeds and required wind speeds do not increase steadily with increasing main span length. Although the reason for this tendency is still under investigation, these long-span cable-stayed bridges with spatial cable planes and steel box girders do not have any problem with aerodynamic instability. The fact that critical flutter speed is relatively insensitive to main span length may support efforts to make another jump in span length of cable-stayed bridges in the near future.

TABLE 10

FUNDAMENTAL NATURAL FREQUENCIES AND FLUTTER SPEEDS OF CABLE-STAYED BRIDGES

Bridge Name	Main Span (m)	Lateral Frequency (Hz)	Vertical Frequency (Hz)	Torsional Frequency (Hz)	Frequency Ratio (Tors/Vert)	Flutter Speed (m/s)	Required Speed (m/s)
Jiangsu Sutong	1088	0.104	0.196	0.565	2.88	88.4	71.6
Stonecutters	1018	0.090	0.184	0.505	2.74	140	79.0
Hubei Edong	926	0.153	0.235	0.548	2.33	81.0	58.6
Tatara	890	0.078	0.139	0.497	3.58	80.0	61.0
Normandy	856	0.151	0.222	0.500	2.25	78.0	58.3

3.3 Rain and Wind Induced Vibration of Stay Cables

The most common problem suffered by the long-span cable-stayed bridges listed in Table 9 relates to the aerodynamics of long stay cables under windy and/or rainy weather conditions. Wind tunnel testing of prototype cable sections was carried out in dry-wind and rain-wind situations, as for example for the Sutong Bridge with outer diameters of 139 mm (the most common cables) and 158 mm (the longest cables). These studies showed that cable vibration is much more severe under the rain-wind condition than under the dry-wind condition for both cable sections shown in Fig. 13, and the maximum amplitudes of these two cables exceed the allowable value of length/1700 (Chen, Lin & Sun, 2004).

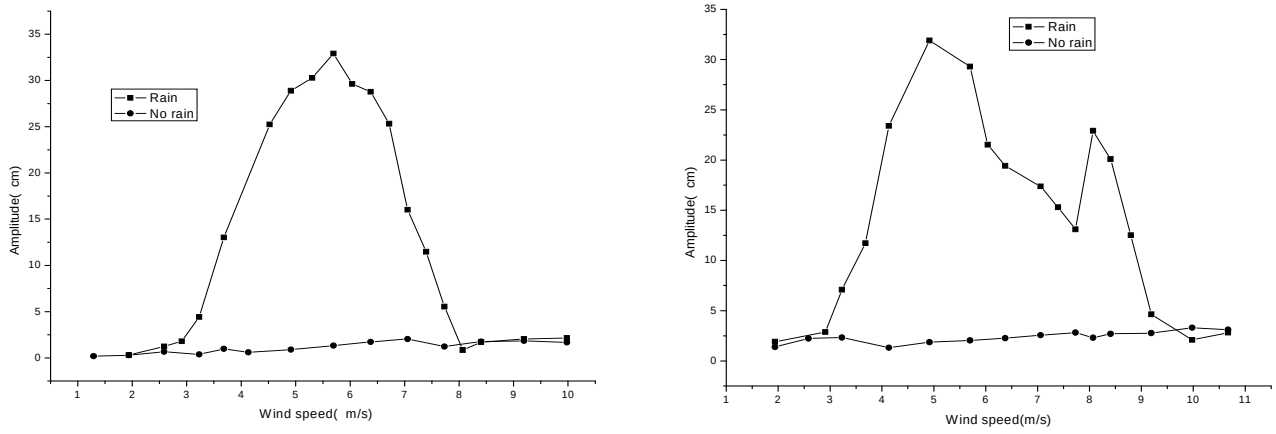

(a) 139 mm dia. stay cable (b) 158 mm dia. stay cable

Figure 13: Cable vibration under dry-wind and rain-wind conditions

The amplitude of rain-wind cable vibration depends on several main factors, one of the most important of which is the spatial cable state, usually described by the angle of inclination of a given cable, α, and the yaw angle of wind flow, β. Fig. 14 gives a comparison of results, from which the most unfavourable spatial state of a 139 mm diameter cable is shown to be at an angle of α = 30°, a yaw angle of β = 35°, and wind speed is between 7 m/s and 11 m/s (Xiang et al., 2005).

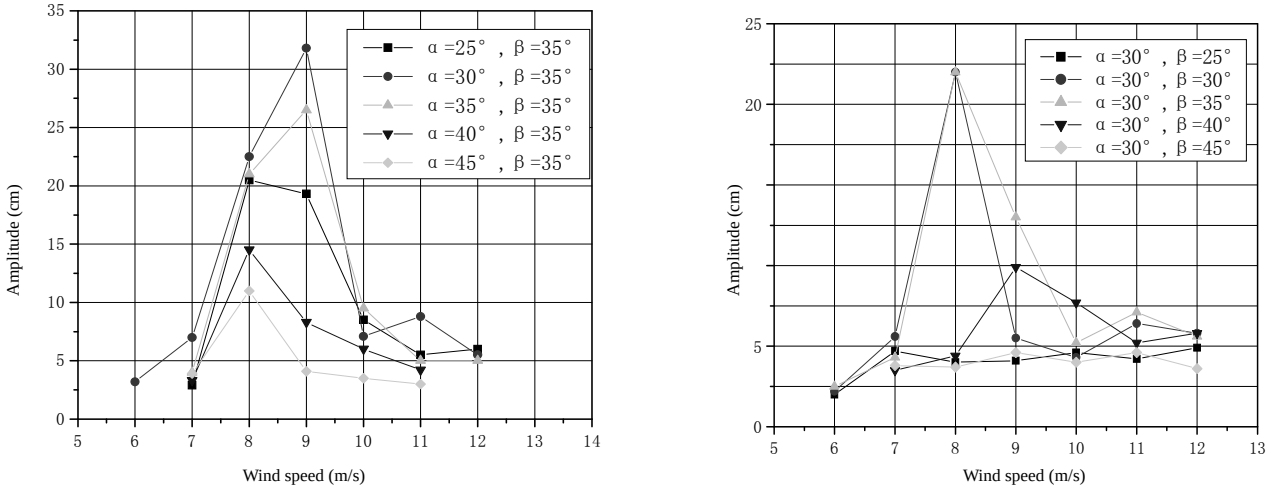

(a) Inclination angle influence (b) Yaw angle influence

Figure 14: Cable rain-wind vibration under different spatial states

In order to reduce severe rain-wind induced cable vibration, cable damping has been investigated together with cable vibration frequency. Based on various on-site measurements of cable damping, the average value of cable damping ratio is found to be about 0.15%. Five damping ratios and four vibration frequencies have been tested. The main results of these tests are presented in Fig. 15. It can be expected that rain-wind induced cable vibration can be effectively controlled by doubling the average damping ratio to 0.30%, which can be accomplished using a variety of damping devices based on different mechanisms, including oil pressure, oil viscous shearing, friction, rubber viscosity, magnetic resistance, electrical resistance, and so on (Xiang et al., 2005).

Another way to ease rain-wind vibration is to prevent the cable surface from forming rivulets, which are known to be the main factor responsible for generating cable vibration. Two kinds of aerodynamic countermeasures, including spiral wires and dimples on the cable surface, were tested and were proven to be effective in reducing vibration amplitude to comply with specified requirements, as shown in Fig. 16. Although cable cross ties are also effective in reducing several types of cable vibration, including rain-wind induced vibration, they have been adopted in only a few cable-stayed bridges including, for example, the Normandy Bridge, one of the ten longest cable-stayed bridges. The lack of applications may be due to the complicated connections to stay cables required by cross ties (Xiang et al., 2005).

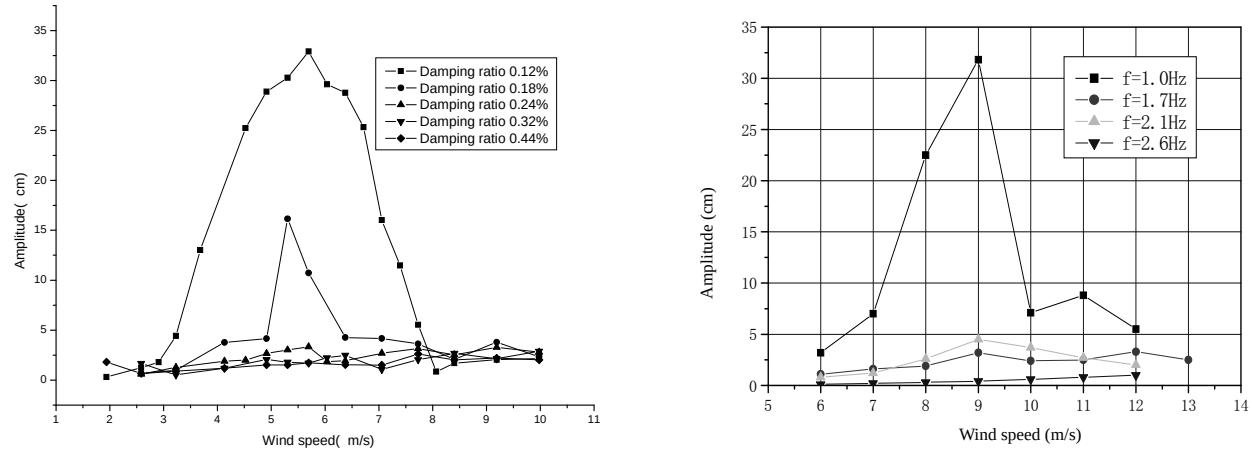

(a) Damping ratio influence (b) Vibration frequency influence

Figure 15: Cable vibration with different damping ratios and frequencies

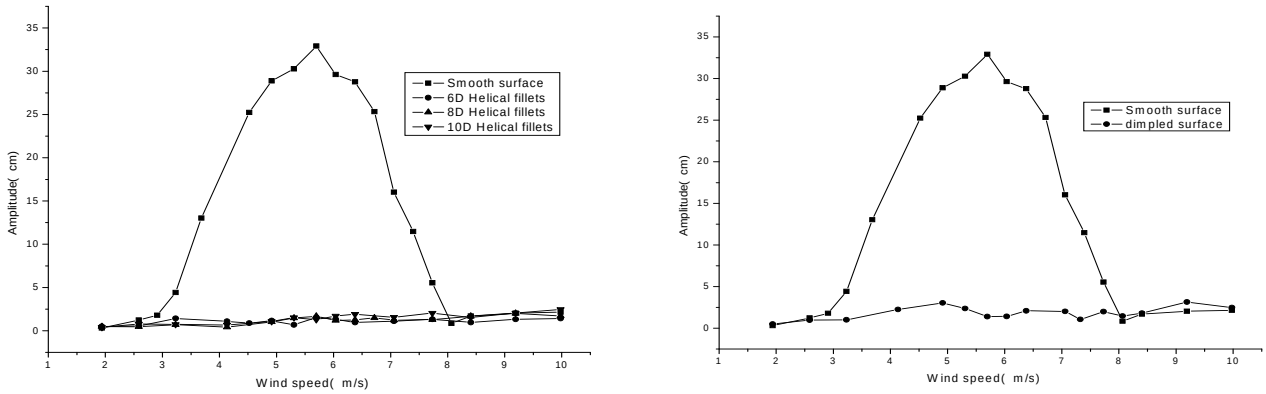

(a) With spiral wires (b) With dimples

Figure 16: Aerodynamic countermeasures of rain-wind induced cable vibration

4. Vortex-Shedding Problems in Arch Bridges

Arch bridges are an ancient bridge type that originated from stone arches, which were first invented around 2500 BC in the Indus Valley Civilization and were known by the ancient Greeks, but developed most fully for bridges by the ancient Romans, some of whose structures still survive. China has a long history of arch bridge construction that dates back some 2 000 years. The oldest existing Chinese arch bridge is the Zhaozhou Bridge of 605 AD, which is the world's first open-spandrel segmental arch bridge to be built completely of stone. In medieval Europe, bridge builders improved on the Roman structures by using narrower piers, thinner arch barrels and lower rise to span ratios. In more modern times, stone and brick arches continued to be built by many civil engineers, but different materials, such as cast iron, steel, and concrete have been increasingly utilized in the construction of arch bridges. The longest arch bridge of the 19th century is Germany's Müngsten Viaduct Bridge with a 170 m main span, which held the world record until the 310 m Hell Gate Bridge built in the USA in 1916. In the 1930's, two famous long-span arch bridges were completed, namely the 504 m Bayonne Bridge in the USA and the 503 m Sydney Harbor Bridge in Australia. These remained the longest spanning arches for 45 years, until completion of the 518 m New River Gorge Bridge in the USA in 1977. In the 21st century, China built several remarkable arch bridges with record-breaking span length, including the 420 m Sichuan Wanxian Bridge as the longest concrete arch, the 460 m Sichuan Wushan Bridge as the longest arch bridge with concrete-filled steel tube arch ribs, the 550 m Shanghai Lupu Bridge as the longest steel arch, and the 552 m Chongqing Caotianmen Bridge which holds the new record for arch span length. The ten longest spanning arch bridges in the world are shown in Table 11. Among these bridges, only one of them, namely the Shanghai Lupu Bridge, suffered wind-induced vibration problems, in this case vortex-shedding oscillation due to the bluff cross sections of arch ribs (Internet address C).

TABLE 11

TEN LONGEST-SPANNING ARCH BRIDGES IN THE WORLD

Span Order	Bridge Name	Main Span	Arch Rib Type	Wind-Induced Problem	Control Measure	Country	Year Built
1	Chongqin Caotianmen	552m	Steel truss	None	None	China	2008
2	Shanghai Lupu	550m	Steel box	Vortex	Cover plate	China	2003
3	New River Gorge	518m	Steel truss	None	None	USA	1977
4	Bayonne	504m	Steel truss	None	None	USA	1931
5	Sydney Harbor	503m	Steel truss	None	None	Australia	1932
6	Sichuan Wushan	460m	Steel tube	None	None	China	2005
7	Guangdong Xinguang	428m	Steel truss	None	None	China	2008
8	Sichuan Wanxian	420m	Concrete box	None	None	China	2001
9	Chongqing Caiyuanba	420m	Hybrid box	None	None	China	2008
10	4th Hunan Xiantan	400m	Steel tube	None	None	China	2007

4.1 Vortex-Induced Vibrations of the Shanghai Lupu Bridge

The Shanghai Lupu Bridge over the Huangpu River is a half-through arch bridge with two side spans of 100 m and a central span of 550 m. The bridge previously held the world record for the longest arch bridge span. The orthotropic steel girder provides six-lane carriageways in the center of the deck and two sightseeing pedestrian ways on both sides, which are supported by arch ribs with hangers and columns. There are eight horizontal post-tensioning tendons in both sides of the girder between the end cross beams to balance the dead load thrust in the central span arch ribs. The entire steel arch-beam hybrid structure is composed of arch ribs, orthotropic girder, inclined hangers and columns, bracings between two ribs, and horizontal post-tensioning tendons as shown in Fig. 17 (SMEDI, 2001).

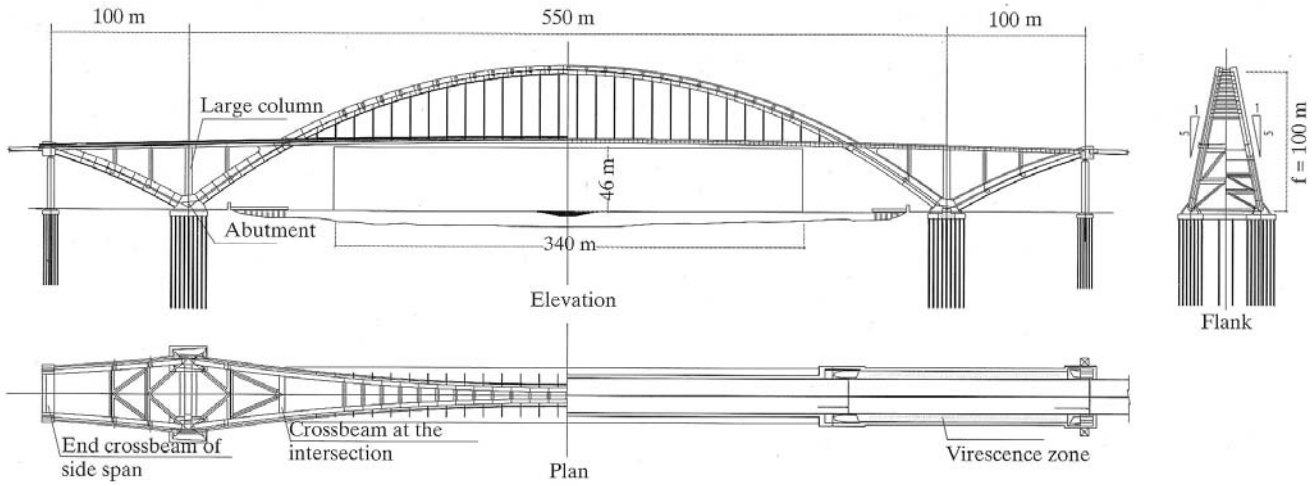

Figure 17: General arrangement of the Shanghai Lupu Bridge (Dimensions in m)

The two inclined arch ribs are 100 m high from the bottom to the crown, and each has the cross section of a modified rectangular steel box with width 5 m, and depth 6 m at the crown and 9 m at the rib bases as shown in Fig. 18. This configuration is susceptible to vortex-induced vibration in the vertical and lateral bending modes of the arch ribs in the completed bridge structure and during construction. Careful aerodynamic investigation of wind induced oscillation of the Lupu Bridge was conducted, based on the particular features of the wind environment around the bridge site in Shanghai, in order to ensure aerodynamic stability and safety of the arch ribs and the whole bridge during construction and after completion. It was found from the investigation that the most unfavorable aerodynamic effect is severe vortex-induced vibration (VIV) of the arch ribs after completion and during construction. In order to avoid severe VIV, some aerodynamic preventive measures were investigated and recommended for implementation (Ge et al., 2002).

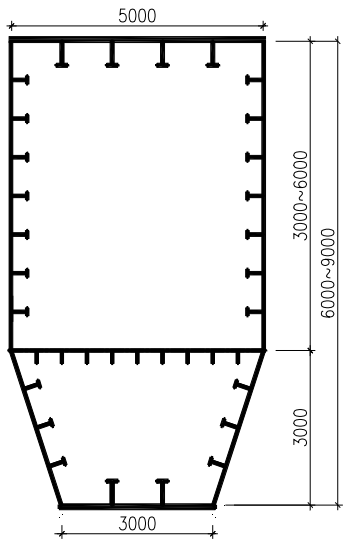

Figure 18: Rib cross section (Dimensions in mm)

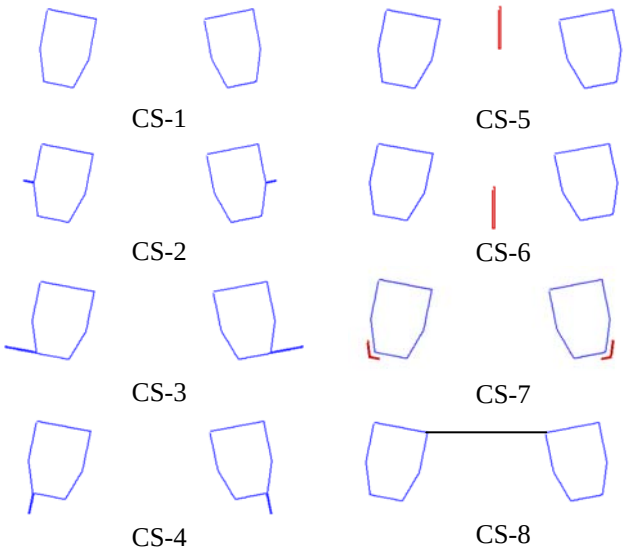

Figure 19: Preventive measures of arch rib against VIV

4.2 Numerical Simulation of Preventive Measures

Although bridge aerodynamics is traditionally investigated through physical testing methods or analytical approaches based on experimentally identified parameters, the application of numerical simulation has become more and more accessible for the aerodynamic design of bridge member geometry and checking of structural performance. Numerical simulation based on computational fluid dynamics (CFD) provides an alternative to physical experimentation such as wind tunnel testing, which often proves to be expensive and time-consuming. As an important example, CFD offers simultaneous determination of force coefficients, pressure distributions, structural response, and flow visualization of structures in various flow fields. This feature in the application of CFD is often helpful and essential for the understanding of the fluid-structure interaction mechanisms that give rise to wind induced vibration.

TABLE 12

STROUHAL NUMBERS AND RELATIVE AMPLITUDES

Case	Rib Configuration	Strouhal	z_{max}/H^*	Reduced
CS-1	Original structure	0.156	0.028	
CS-2	2m middle plates	0.220	0.025	11%
CS-3	2m bottom plates (H)	0.137	0.034	
CS-4	2m bottom plates (V)	0.137	0.032	
CS-5	4m top stabilizer	0.137	0.032	
CS-6	4m bottom stabilizer	0.156	0.017	39%
CS-7	4m corner deflectors	0.175	0.023	18%
CS-8	Full cover plate	0.156	0.011	61%

* z_{max} is the maximum VIV amplitude, and H is the rib depth.

The random vortex method code RVM-FLUID (Zhou, 2002) developed in Tongji University in 2002 was used to analyze a two-dimensional model of a pair of rib cross sections with an average depth of 7.5m. It was found that severe VIV happens with an amplitude of 0.028H (rib depth) at the Strouhal number (reduced frequency) S_t = 0.156. In order to improve resistance to VIV of the bluff cross section of the ribs, the aerodynamic preventive measures shown in Fig. 19 were numerically investigated. The calculation results including Strouhal numbers and relative amplitudes are listed in Table 12. There are only four effective schemes of preventive measures, including CS-2, CS-6, CS-7 and CS-8, which can reduce the amplitude of VIV to some extent. Among these four schemes, the best solution is the scheme of the full cover plate (CS-8), which can reduce the amplitude to only about 40% of that in the original configuration (Ge & Xiang, 2004).

4.3 Wind Tunnel Testing Confirmation of Effective Preventive Measures

The aeroelastic model used to confirm the effectiveness of the full cover plate was designed with a linear scale of 1:100 of the prototype structure with the entire model simulated in sufficient detail, including anti-collision walls and other deck details. Apart from Reynolds number, the similarities of the other dimensionless quantities were carefully adjusted. The full aeroelastic model of the Lupu Bridge was designed and constructed for the structure configurations corresponding to three construction stages, the maximum rib cantilever (MRC), the completed arch rib (CAR), and the completed bridge structure (CBS). The wind tunnel experiments of VIV with aeroelastic models were carried out in the TJ-3 Boundary Layer Wind Tunnel as shown in Fig. 20 (Ge et al., 2002).

Several wind tunnel testing cases were conducted for three bridge configurations with or without preventive measures under different angles of attack and different yaw angles. The measured data include the displacements of arch ribs and stiffening girder at mid-span (L/2) and quarter span (L/4) of the centre span, and the displacements at the top of one temporary tower. Due to the bluff feature of the arch rib sections, significant VIV oscillation was observed in vertical and lateral bending modes during testing. Two schemes of aerodynamic preventive measures were experimentally investigated, including the full cover plate between two arch ribs (scheme A) and a partial cover plate with 30% air vent (scheme B). The main experimental results including the maximum displacements of vertical and

lateral VIV of the arch ribs at mid span ($L/2$) and quarter span ($L/4$) are listed in Table 13. It can be concluded that scheme A or B effectively makes it possible to reduce VIV amplitudes (Ge et al., 2002).

Figure 20: Aerodynamic model of the Shanghai Lupu Bridge

TABLE 13

MAXIMUM VIV AMPLITUDES OF ARCH RIBS AND CORRESPONDING WIND SPEEDS

Bridge Configuration	Attack Angle	Control Measures	Speed (m/s)	Frequency (Hz)		L/2 Amplitude (m)		L/4 Amplitude (m)	
				Vertical	Lateral	Vertical	Lateral	Vertical	Lateral
Maximum Rib Cantilever (MRC)	0°	Original	16.3	0.393	0.408	0.813	0.308	0.216	
			26.3	0.393	0.408	0.656	0.272	0.176	
		Scheme A	17.5	0.393	0.408	0.590	0.237	0.166	
			25.0	0.393	0.408	0.333	0.144	0.100	
		Scheme B	16.3	0.393	0.408	0.249	0.115	0.069	
			42.5	0.883	0.408	0.374	0.195	0.262	0.082
Completed Arch Ribs (CAR)	+3°	Original	31.3	0.679	0.441	0.115		0.634	
		Sch. A	33.8	0.679	0.441	0.066	0.074	0.358	
		Sch. B	31.3	0.679	0.441	0.047	0.055	0.359	
Completed Bridge Structure (CBS)	-3°	Original	17.5	0.368		0.040		0.164	
			35.0	0.368		0.135		0.588	
		Scheme A	17.5	0.368		0.067		0.070	
			32.5	0.368		0.047		0.239	
		Scheme B	17.5	0.368		0.067		0.023	
			32.5	0.368		0.037		0.203	

5. Conclusions and Prospects

Several types of long-span bridges, namely suspension bridges, cable-stayed bridges, and arch bridges, have been ranked according to length of main span. The top ten bridges of each type have been investigated for wind-induced problems, including aerodynamic instability, rain-wind induced vibration of stay cables, and vortex-induced vibration. Through research and continuous development, the prospects for increasing span length and aerodynamic performance of suspension bridges, cable-stayed bridges, and arch bridges have been evaluated.

Based on the experience gained from recently built suspension bridges, such as the Akashi Kaykyo, Zhejiang Xihoumen, Great Belt, Jiangsu Runyang and Tsing Ma bridges, the intrinsic limit of span length due to aerodynamic stability has been determined to be about 1 500 m for traditional suspension bridges with either a streamlined box deck or a ventilative truss girder. Beyond or even approaching this limit, designers should be prepared to improve aerodynamic stability of bridges by modifying the cable system or adopting countermeasures in the girder, including vertical and/or horizontal stabilizers and slotted deck, as well as passive and active control devices. Based on a preliminary study, either a widely slotted deck or a narrowly slotted deck with vertical and horizontal stabilizers could provide a 5 000 m span-length suspension bridge with a sufficiently high critical wind speed to satisfy aerodynamic requirements in most typhoon-prone areas in the world.

The practice of the latest record-breaking cable-stayed bridges, such as the Jiangsu Sutong, Stonecutters, Hubei Edong, Tatara, and Normandy bridges, demonstrates that long span cable-stayed bridges with spatial cable planes and steel box girders have sufficiently high critical flutter speed and the main aerodynamic concern on this type of structure is rain-wind induced vibration of long stay cables. It seems that there is still room to increase main span length of cable-stayed bridges with regard to aerodynamic stability. With the development of effective solutions for cable vibration mitigation, further increases in span length can be expected in cable-stayed bridges in the near future.

The span length of arch bridges has not grown as fast as suspension bridges and cable-stayed bridges, and structural stiffness has likewise not decreased as much as the other two types of bridge. Based on the evidence that only one out of the ten longest-span arch bridges was susceptible to vortex-induced problems, the enlargement of span length of arch bridges should not be influenced by aerodynamic requirements, but rather by other aspects, for example, static instability, horizontal thrust, and construction technology.

References

- Chen A.R., Guo Z.S., Zhou Z.Y., Ma R.J and Wang D.L. (2002). Study of Aerodynamic Performance of Runyang Bridge, *Technical Report WT200218*, State Key Laboratory for Disaster Reduction in Civil Engineering at Tongji University (in Chinese)
- Chen A.R., Lin Z.X. and Sun L.M. (2004). Testing and Study on Wind/Rain Vibration, Force Optimisation and Vibration Mitigation of Stay Cables of Sutong Bridge, *Technical Report WT 200419*, State Key Laboratory for Disaster Reduction in Civil Engineering at Tongji University (in Chinese)
- China Highway Planning and Design Institute (2003). *Preliminary Design Drawings of Xihoumen Bridge* (in Chinese)
- Falbe-Hansen K., Hauge L. and Kite S. (2004). Stonecutters Bridge – Detailed design, *Proceedings of the IABSE Symposium 2004 on Metropolitan Habitats and Infrastructure*, Shanghai, China, September 22-24
- Ge Y.J., Cao F.C., Pang J.B. and Yang Y.X. (2002). Study of Aerodynamic Performance and Wind Loading of Shanghai Lupu Bridge, *Technical Report WT200103*, State Key Laboratory for Disaster Reduction in Civil Engineering at Tongji University (in Chinese)
- Ge Y.J., Yang Y.X., Cao F.C. and Zhao L. (2003). Study of Aerodynamic Performance and Vibration Control of Xihoumen Bridge, *Technical Report WT200320*, State Key Laboratory for Disaster Reduction in Civil Engineering at Tongji University (in Chinese)
- Ge Y.J. and Xiang H.F. (2004). Recent development of bridge aerodynamics in China, *Keynote Paper in Proceeding of the 5th International Colloquium on Bluff Body Aerodynamics and Applications*, Ottawa, Canada
- Ge Y.J. and Xiang H.F. (2006a). Outstanding Chinese steel bridges under construction, *Proceedings of the 6th International Symposium on Steel Bridges*, Prague, Czech Republic, June 1-3
- Ge Y.J. and Xiang H.F. (2006b). Tomorrow's challenge in bridge span length, *Proceedings of the IABSE Symposium 2006 on Responding to Tomorrow's Challenges in Structural Engineering*, Budapest, Hungary, September 13-15, 1000-1010.
- Ge Y.J. and Xiang H.F. (2007). Great demand and various challenges - Chinese Major Bridges for Improving Traffic Infrastructure Nationwide, *Keynote paper in Proceedings of the IABSE Symposium 2007 on Improving Infrastructure Bringing People Closer Worldwide*, Weimar, Germany, September 19-21, 9-12.
- Internet address A (2007), http://en.wikipedia.org.wiki//List_of_longest_suspension_bridge_spans
- Internet address B (2007), http://en.wikipedia.org.wiki//List_of_the_largest_cable-stayed_bridges
- Internet address C (2007), http://en.wikipedia.org.wiki//List_of_the_largest_arch_bridges
- Pei M.S., Zhang X.G., Yuan H. and Xu L.P. (2004). Design of Superstructure for Sutong Bridge, *Paper*

Collecting of Sutong Bridge (No. 1), Sutong Bridge Construction Commanding Department, Chinese Science and Technology Press (in Chinese)

- Shanghai Municipal Engineering Design Institute (SMEDI). (2001). *Detailed Design Drawings of Shanghai Lupu Bridge* (in Chinese)
- Song J.Z., Xu J.Y., Ge Y.J. and Zhu L.D. (2005). Wind Tunnel Study of Edong Bridge with Aeroelastic Model, *Technical Report WT200708*, State Key Laboratory for Disaster Reduction in Civil Engineering at Tongji University (in Chinese)
- Xiang H.F., Chen A.R and Ge Y.J. (2003). *Major Bridges in China*, China Communications Press, Beijing, China
- Xiang H.F. and Ge Y.J. (2003). On aerodynamic limit to suspension bridges, *Proceedings the 11th International Conference on Wind Engineering*, Texas, USA, June 2-5
- Xiang H.F., Ge Y.J., Zhu L.D., and et al. (2005). *Modern Wind-Resistant Theory and Practice of Bridges*, China Communications Press, Beijing, China (in Chinese)
- Zhou Z.Y. (2002). Numerical calculation of aeroelastic problems in bridge by random vortex method, *Post-doctoral Research report*, Tongji University, China (in Chinese)